Design and Application of Hybrid Magnetic Field-Eddy Current Probe

Buzz Wincheski[a], Terryl Wallace[a], Andy Newman[a], Paul Leser[a], and John Simpson[b]

[a]NASA Langley Research Center, Hampton VA, 23681
[b]Northrop Grumman, Hampton VA, 23681

Abstract. The incorporation of magnetic field sensors into eddy current probes can result in novel probe designs with unique performance characteristics. One such example is a recently developed electromagnetic probe consisting of a two-channel magnetoresistive sensor with an embedded single-strand eddy current inducer. Magnetic flux leakage maps of ferrous materials are generated from the DC sensor response while high-resolution eddy current imaging is simultaneously performed at frequencies up to 5 MHz. In this work the design and optimization of this probe will be presented, along with an application toward analysis of sensory materials with embedded ferromagnetic shape-memory alloy (FSMA) particles. The sensory material is designed to produce a paramagnetic to ferromagnetic transition in the FSMA particles under strain. Mapping of the stray magnetic field and eddy current response of the sample with the hybrid probe can thereby image locations in the structure which have experienced an overstrain condition. Numerical modeling of the probe response is performed with good agreement with experimental results.

Keywords: Eddy Current, Anisotropic Magnetoresistance, Ferromagnetic Shape Memory Alloy
PACS: 81.70.Ex, 81.05.Bx, 81.30.Kf

INTRODUCTION

Eddy current probes based upon magnetic field sensors have been shown to have many potentially advantageous attributes in the past [1-5]. Much work has focused on the low-frequency capabilities of Hall probes and magneto-resistive sensors to develop low frequency eddy current devices with deep flaw detection capabilities [1-3]. More recently, the small form factor of many solid-state magnetic field sensors has been investigated for high-resolution imaging using scanned sensors or high-density sensor arrays [4,5]. In one such example a two-axis orthogonal magnetoresistive sensor based eddy current probe developed by our group was shown to isolate features separated by as small as 250 μm while also measuring stray DC magnetic fields with sub-mOe resolution [5,6]. Continued work on this sensor platform has resulted in increased functionality through a redesign of the induction wire path. In addition, concurrent acquisition of DC magnetic field and high frequency eddy current signals is demonstrated. The resulting hybrid magnetic field-eddy current probe is capable of producing high spatial resolution imaging of both the stray magnetic field and eddy current response in a single scan. Along with the probe design, an application toward analysis of a sensory material consisting of an aluminum alloy with embedded ferromagnetic shape memory alloy particles is presented. In addition, finite element modeling of the probe response is performed to aid in the understanding of the probe operation. Experimental data for inspection of sensory alloy materials under investigation at NASA LaRC are presented and compared with finite element modeling predictions.

DESIGN OF HYBRID MAGNETIC FIELD-EDDY CURRENT PROBE

The hybrid magnetic field-eddy current probe is designed upon a commercially available two-axis anisotropic magnetoresistive (AMR) sensor with a reported bandwidth of 5 MHz (DC to 5 MHz), resolution of 27 μgauss, and linear output with field from -2 to 2 gauss at a sensitivity of 3 mv/V/Oe [7]. The solid-state chip has a footprint of roughly 7 mm x 12.7 mm (active area of each sensor element ~ 250 μm^2) and operates between -55 and 150 degrees C. This combination of attributes is well suited for many nondestructive evaluation magnetic field mapping applications and requires only an induction source to perform as an eddy current probe. In previous work we have discussed the use of a single-strand induction wire placed directly below the active elements to maximize the spatial resolution of the eddy current signature [5]. As noted in that work, the designed induction wire placement

introduced an artifact in the eddy current imaging with features being elongated along the current flow direction. Although image processing was shown to significantly reduce this artifact, an alternate induction wire path was studied here as a means to improve the quality of the raw data.

Figure 1 displays the design of the new induction wire path along with the location and sensing axis of the two AMR elements within the sensor chip. In operation the chip is positioned such that the induction wire is adjacent to and parallel with the sample surface. Channels .008" deep x .006" wide are cut directly into the face of the chip to guide the induction wire placement and protect the wire during use. Care was taken in designing the wire placement path to avoid long straight current flows in the area of the AMR elements and to compensate current flows with cancelation currents to the maximum extent possible. The resulting current distribution produces a dipole like magnetic field aligned with and directly above the sensing axis of the underlying AMR elements and reduces the spreading artifact seen in the previous prototype.

As the AMR magnetic field sensors have micro-gauss resolution only small currents are needed to act as an induction source. This allowed experimental work to be performed using an unamplified general-purpose function generator as the driver. The coil current, calculated as the voltage drop across the induction wire divided by the sensor impedance, was found to be ~ 70 mA rms. The magnetic field at the sensor location can be calculated using Ampere's law, given in CGS units by:

$$\nabla \times H = \frac{4\pi}{c} J.$$ (1)

The field at the sensor with the probe operating in air reduces to:

$$H = 0.2 * J / r,$$ (2)

where H is the magnetic field in Oe, J is the induction wire current in amps, and r is the distance between the induction wire and the AMR element in centimeters. Estimating the spacing between the induction wire and the AMR element at 0.5 mm yields a magnetic field of 0.28 Oe at the AMR element when the probe operates in air. Experimental measurements for this operating condition find the magnetic field to be approximately 0.23 Oe, suggesting that the actual induction wire to AMR element spacing is closer to 0.6 mm. X-ray images of the sensor cross section confirm that this measurement is consistent with the distance of the AMR elements beneath the surface of the sensor.

FINITE ELEMENT MODELING

Three-dimensional finite element modeling for a simplified inspection geometry is displayed in figure 2. All finite element modeling results were acquired using the COMSOL multi-physics AC/DC package. The model has been constructed to calculate the probe response to an embedded hemispherical ferromagnetic object in an aluminum matrix, with physical significance to be discussed later. Only the area very near the AMR element is modeled, such that the induction wire can be approximated as an infinitely long straight current. A 0.2 mm
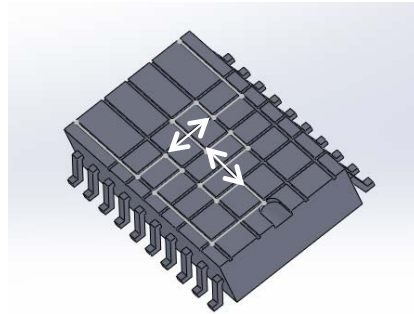

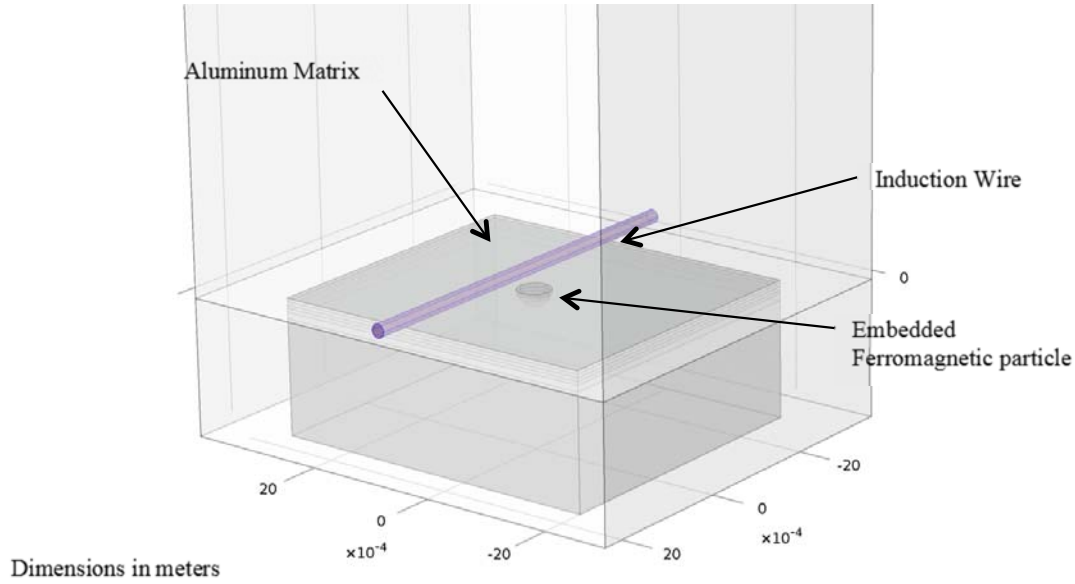**FIGURE 1.** Induction wire placement and sensing axes of anisotropic magnetoresistive sensor

FIGURE 2. Three-dimensional finite element model of sensor interaction with embedded ferromagnetic particle.

diameter induction wire is placed with a standoff of 0.1 mm above the aluminum sample. The top layers of the aluminum plate and the embedded ferromagnetic particle have been discretized into thin layers to force a high-density mesh near the sample surface to account for skin depth effects. The ferromagnetic particle is modeled as an iron hemisphere of 0.5 mm diameter, co-planar with the sample surface. The calculations are performed at an operating frequency of 1 MHz, and the data are processed to extract the magnetic field at the location of the AMR element (0.6 mm above the wire center, as discussed above).

Figure 3 shows line profiles for the calculated response of the probe for scans directly centered on the ferromagnetic particle, 0.25 mm off-center, and 0.5 mm off-center from the particle. In each scan the current flow
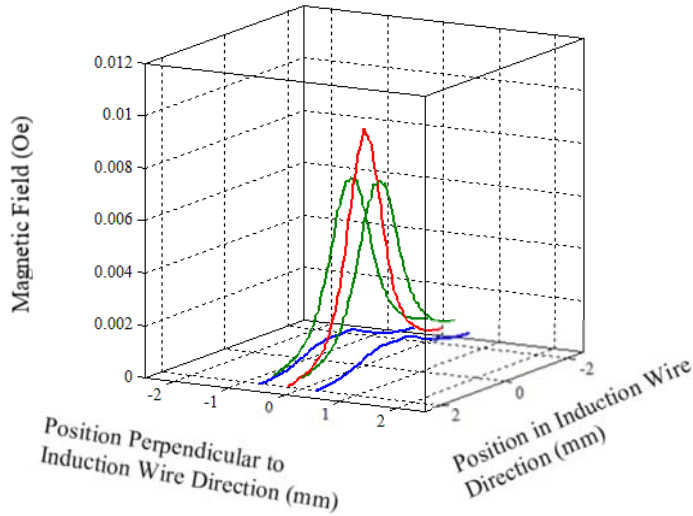

FIGURE 3. Finite element modeling results for the sensor response to embedded ferromagnetic particle.

direction is along the continuous scan line, the field is measured in the perpendicular direction, and the particle is centered at the (0,0) location. A peak field is calculated when the probe is centered on the ferromagnetic particle, with an increase in the field level of 9 mOe as compared to the aluminum matrix material. This field change is more than two orders of magnitude above the stated resolution of the sensors. The fields are also seen to rapidly drop to background levels with distance away from the particle, enabling discrimination of the effect of individual particles in a composite system.

EXPERIMENTAL TESTING

The sensor chip pictured in figure 1 is configured into an inspection system using the schematic diagrams shown in figure 4. Two potential configurations have been tested. In figure 4a, a continuous wave source is used to drive the induction wire. The output signal from the AMR sensor is split into two paths. In the first, a low pass filter is applied and the low frequency magnetic field component due to stray fields in the part under test is recorded. In the second path, the signal is fed into a lock-in amplifier referenced to the drive source, enabling the amplitude and phase of the signal at the induction current frequency to be monitored. Figure 4b displays a second data acquisition methodology. In this configuration a tone burst source is used to drive the induction wire and a full waveform capture of the AMR sensor response is performed. Amplitude and phase information at the tone burst frequency are calculated from the Fast-Fourier Transform of the acquired waveform. FFT analysis is also used to examine overtone frequencies and the low frequency stray magnetic field component of the signal. As reported in earlier work, the clock signal is also correlated with motion control devices for enhanced spatial resolution [5]. Incorporation of a high-speed data acquisition board enables extremely fast data acquisition and storage.

Experimental testing of the hybrid probe was performed on a sensory alloy under development at NASA LaRC [8]. The alloy consists of an aerospace aluminum host matrix embedded with ferromagnetic shape memory alloy (FSMA) particles. Under strain, the FSMA particles are designed to undergo an austenitic to martensitic transformation. In addition to energy release through acoustic emission, a change in the electromagnetic properties
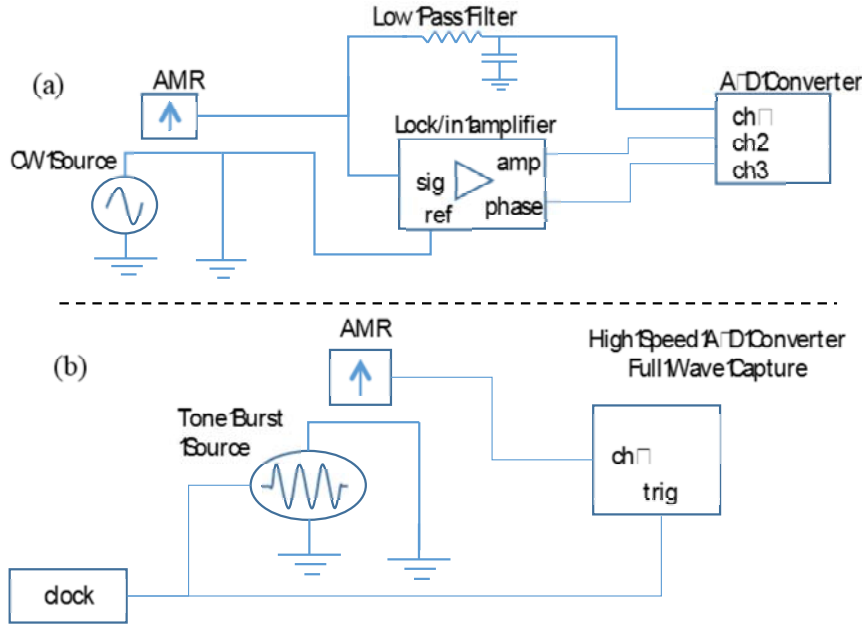

FIGURE 4. Drive and data acquisition circuitry for (a) lock-in amplifier and (b) full waveform capture modes of operation. Duplicate circuitry for second AMR measurement axis not shown for simplicity.

of the FSMA particles occurs [6]. Noninvasive measurements of the electromagnetic properties of the embedded FSMA particles can thereby be used to infer the strain state of the structure. Testing of the hybrid magnetic field-eddy current sensor on the sensory alloy was designed to see if the electromagnetic properties of individual FSMA particles could be analyzed, providing a path toward rapid and nondestructive strain mapping in aerospace components.

Figure 5 displays eddy current and stray magnetic field C-scan plots for an experimental sensory alloy as discussed above using a NiFeGa alloy as the embedded FSMA. The x-axis and y-axis eddy current plots in figure 5a and 5b highlight individual near-surface FSMA particles. The higher permeability and lower conductivity of the FSMA particles as compared to the host aluminum alloy matrix produce the measured contrast in the image. The magnitude of the change in magnetic field across the particles is on the order of 10 mOe, consistent with the finite element modeling results shown in Figure 3. An elongation of the features along the local current flow direction (perpendicular to magnetic field measurement direction) is also observed, although the effect is significantly reduced as compared to the previous prototype probe design [5].

In figures 5c and 5d the stray magnetic field across the sample in the x and y directions is plotted. The data, acquired with the sample in a demagnetized state, show artifacts from several particles with remanent magnetic field. The largest measured stray field is on the order of 200 mOe, associated with a particle in the upper left corner of the images. To more closely study the magnetic behavior of the embedded particles, the sample was placed in a uniform magnetic field of 8 kOe along the x-axis of the sample. The field was then reduced to zero and the stray magnetic field data re-acquired. The resulting data are displayed in figure 6. As expected a much larger remanent field is detected. The field near the artifact observed in figure 5 is now seen to exceed 2 Oe, surpassing the dynamic range of the sensor. Note that a larger scan area is displayed in figure 6 as compared to figure 5 with the high amplitude feature of figure 5 roughly centered along the x-axis in figure 6. Many other particles with remanent field aligned along the magnetization direction are also evident in figure 6. It is interesting to note that most of the particles detected in figures 5a and 5b by eddy current imaging are not apparent in the magnetic field images of figures 5c and 5d or 6a and 6b. The low stray magnetic field of these particles as compared to those detected in the magnetic field images suggests that the particles have a much lower remanent magnetization. Although further testing is required to verify and isolate the cause for the difference in magnetic properties of the various particles in
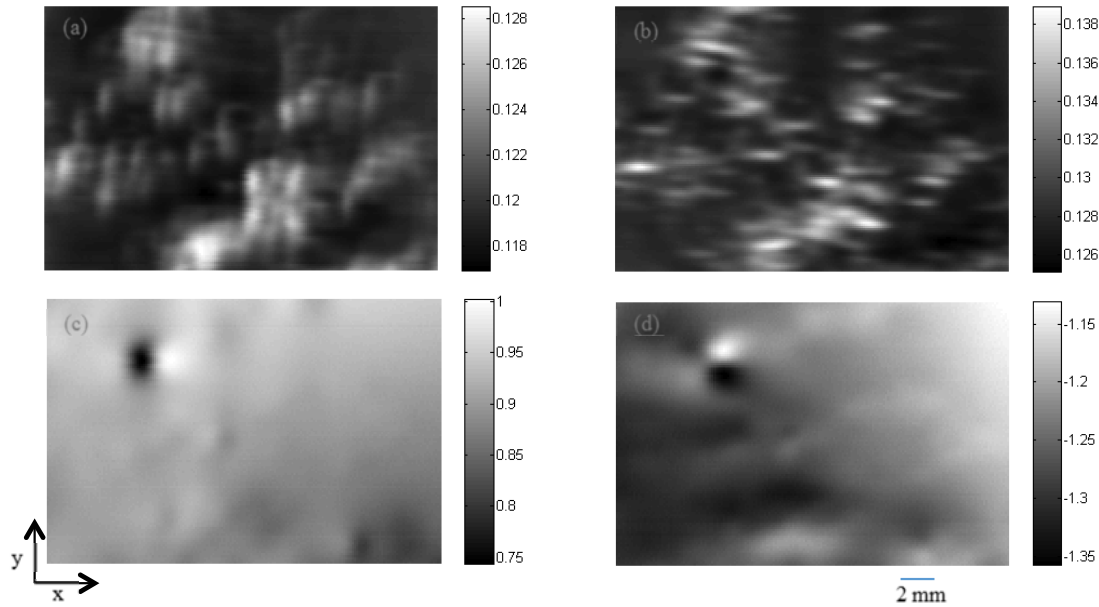

FIGURE 5. Hybrid magnetic field-eddy current probe response for sensory alloy with embedded ferromagnetic shape memory alloy particles in aluminum matrix. Images show C-scan results for eddy current/stray magnetic field response in x (a)/(c) and y (b)/(d) directions. All c-scans represent the same area of the sample. Color bar units are in Oersted.
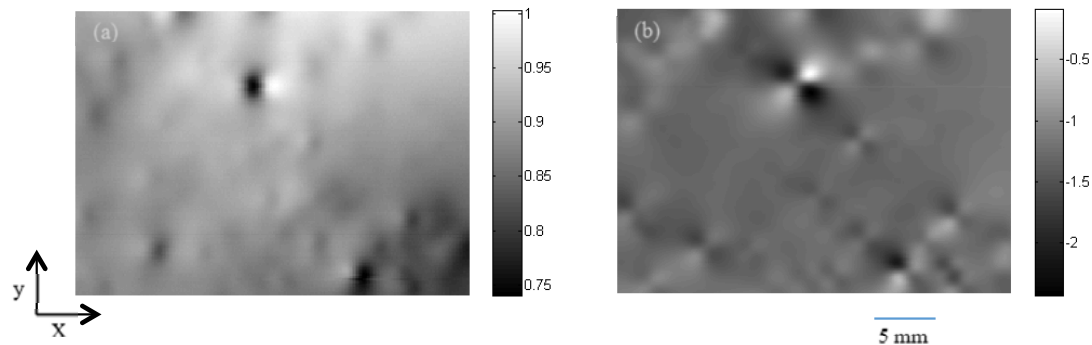
FIGURE 6. C-scan results for stray magnetic field response in x (a) and y (b) directions for sample imaged in figure 5 after the sample was subject to a magnetizing field in the x-direction. C-scans represent the same area of the sample and color bar units are in Oersted.

the sample, the experimental data verify that the electromagnetic properties of individual FSMA particles can be interrogated using the hybrid magnetic field–eddy current probe. Such a capability is a critical first step to strain mapping in a sensory alloy composed of FSMA particles.

A last experimental example of imaging of FSMA particles with the hybrid probe is shown in Figure 7. The C-scan images map the stray magnetic field for a sensory alloy containing NiMnGa FSMA particles. Figure 7a and 7b display the stray field in the x and y directions after the sample was subject to a magnetizing field of 8 kOe in the x-direction in the manner described in relation to figure 6. Figure 7c and 7d show the corresponding images after the sample was demagnetized. In contrast to the data for the NiFeGa sample, the magnetized sample shows a complicated pattern as the stray fields of the network of embedded NiMnGa particles interact. The data suggest that the particles have a relatively high but uniform remanence. Upon demagnetizing of the sample the stray magnetic field images are significantly de-cluttered. Only a handful of individual particles contribute to the measured fields with the stray field patterns of figure 7c and 7d consistent with an out-of-plane magnetization of the detected particles.

SUMMARY

A hybrid magnetic field-eddy current probe has been developed based upon the sensing capabilities of a two-axis anisotropic magnetoresistive sensor. The hybrid probe measures in-plane static and dynamic magnetic fields at frequencies up to 5 MHz. The incorporation of a single strand inducion wire produces eddy current imaging capabilities. The induction wire path is designed to localize the effects of the induction current at the AMR sensor elements for improved localization of the eddy current response. The capabilities of the probe in both static magnetic field and eddy current imaging have been demonstrated in the characterization of a sensory alloy containing embedded ferromagnetic shape memory alloy particles in an aluminum matrix. A martensitic transformation of the embedded FSMA particles with strain is anticipated to result in changes to the electromagnetic properties of the particles, potentially including permeability, resistivity, saturation magnetization, coercive field, and remanent magnetization. Measurement of some or all of these properties can then be used as a means to analyze the stress distribution in the material. The presented data have shown that the hybrid probe can isolate individual FSMA particles based upon the eddy current response and stray magnetic field distribution of the particles, with experimental data correlating well with finite element modeling predictions. Continued work is in progress to determine whether a strain-induced martensitic transformation of the embedded FSMA particles can be isolated in the data. A parallel ongoing effort is focused on optimizing the FSMA to maximize magnetic property changes due to a strain-induced martensitic transition. A successful mating of these two efforts has the capability of enabling nondestructive mapping of the stress distribution in aerospace components.
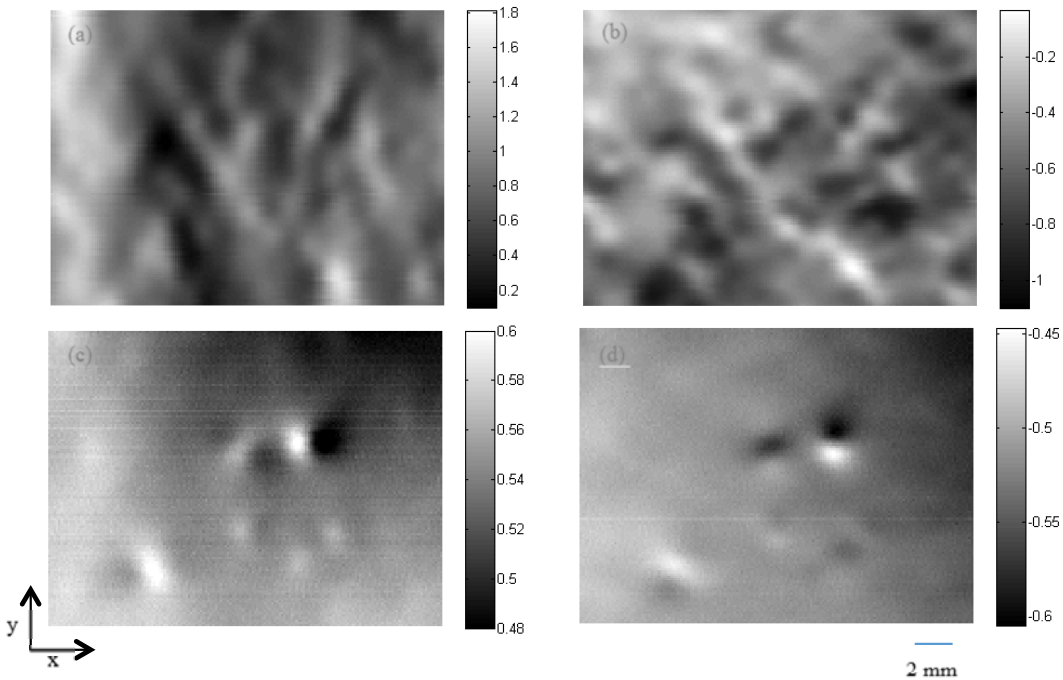
FIGURE 7. C-scan results for stray magnetic field response in x (a & c) and y (b & d) directions for NiMnGa based sensory alloy after sample was subject to magnetizing field in x-direction (a & b) and following demagnetization (c & d). C-scans represent the same area of the sample and color bar units are in Oersted.

REFERENCES

1. B. Wincheski and M. Namkung, "Deep Flaw Detection with Giant Magnetoresistive (GMR) based Self-Nulling Probe," in *Review of Progress in Quantitative NDE*, Vol. 19, pp. 465-472, 2000.
2. Gui Yun, T., et al. (2005). "Multiple sensors on pulsed eddy-current detection for 3-D subsurface crack assessment." Sensors Journal, IEEE **5**(1): 90-96.
3. D. Motes, J.C. Aldrin, M. Keiser, G. Steffes, and D.S. Forsyth, "GMR sensing array technique for the inspection of multi-layer metallic structures," AIP Conf. Proc. 1511, pp. 1562-1569, *Review of Quantitative Nondestructive Evaluation*, 2013.
4. Nazarov, A. V., et al. (2004). "Arrays of magnetoresistive sensors for nondestructive testing." Journal of Vacuum Science & Technology A: Vacuum, Surfaces, and Films **22**(4): 1375-1378.
5. B. Wincheski and J. Simpson, J.P. Seebo, and J. Powell, "High resolution imaging with two-axis orthogonal magneto-resistive sensor based eddy current probe," in *Review of Progress in Quantitative NDE*, Vol. 31, pp. 366-372, 2012.
6. B. Wincheski, J. Simpson, T. Wallace, A. Newman, P. Leser, and R. Lahue, "Electromagnetic Characterization of Sensory Alloy," AIP Conf. Proc. Vol. 1511, pp. 1547 – 1554, *Review of Quantitative Nondestructive Evaluation*, 2013.
7. Honeywell Sensor Products, 1- and 2-axis Magnetic Sensors, MHC1001/1002 HMC1021/1022, www.magneticsensors.com, 900248 Rev. B.
8. T. Wallace, J. Newman, M. Horne, and P. Messick, "Development of Metallic Sensory Alloys," in *Materials Science and Technology 2010*, NASA Aeronautics and Space Database, CASI 20100038432, 2010.